Microstructural study of Mg-Zn alloys prepared by mechanical alloying

A.F. Palacios-Lazcano, J.L. Luna-Sánchez,
F. Cruz-Gandarilla, and J.G. Cabañas-Moreno*
Instituto Politécnico Nacional, ESFM, Depto. de Ciencia de Materiales,
Edif. No.9, UPALM, 07338, México, D.F.,
e-mail: apalacios@esfm.ipn.mx, jjjluis@tutupia.com,
fcruz@esfm.ipn.mx, gcabanas@esfm.ipn.mx

M. Umemoto
Department of Production Systems Engineering, Toyohashi University of Technology,
Toyohashi, Aichi 441-8580, Japan,
e-mail: umemoto@martens.tutpse.tut.ac.jp

Recibido el 7 de julio de 2006; aceptado el 7 de diciembre de 2006

Elemental powder mixtures of Mg (particle size < 500 μm) and Zn (< 100 μm) have been subjected to mechanical alloying (MA) in a planetary ball mill in order to produce suitable hydrogen storage alloys. Milling parameters such as ball-to-powder mass ratio and milling time have been varied to secure the production of homogeneous nanocrystalline Mg-Zn alloyed powders containing 5 and 10 wt.% Zn. Characterization of the alloys thus produced has been carried out by X-ray diffraction, scanning electron microscopy, elemental microanalysis and transmission electron microscopy. It is demonstrated that the mechanically alloyed powders are metastable Mg-Zn solid solutions with a nanocrystalline structure and a homogeneous composition after MA.

Keywords: High-energy ball milling; nanocrystalline materials; metastable phases; Magnesium-base alloys; mechanical alloying.

Mezclas de polvos elementales de Mg (tamaño de partícula < 500 μm) y Zn (< 100 μm) han sido sometidas al proceso de aleado mecánico en un molino planetario de alta energía. Los parámetros del proceso de molienda, tales como la razón de masa de bolas a masa de polvos y el tiempo de molienda, han sido optimizados a fin de obtener polvos nanocristalinos de aleaciones homogéneas Mg-Zn, con contenidos de Zn de 5 y 10% peso. La caracterización de las aleaciones así producidas ha sido realizada mediante difracción de rayos X, microscopía electrónica de barrido, microanálisis químico elemental y microscopía electrónica de transmisión. Se demuestra que los polvos mecánicamente aleados son soluciones sólidas Mg-Zn que poseen una estructura nanocristalina y una composición homogénea después el aleado mecánico.

Descriptores: Molienda mecanica de alta energia; materiales nanocristalinos; fases metaestables; aleaciones base Magnesio; aleado mecanico.

PACS: 81.07.Bc, 81.20.Ev, 64.60.My

1. Introduction

Mg-based alloys are of importance as hydrogen storage materials because Mg possesses a low density, is relatively cheap and has one of the highest hydrogen storage capacities (~ 7.6 wt.%) in solid materials [1]. On the other hand, it has been found [2-4] that nanocrystalline alloys and compounds show faster hydriding and dehydriding kinetics in comparison to their conventional polycrystalline counterparts, probably due to their more numerous grain boundaries and lattice defects which can serve as fast diffusion paths for hydrogen mobility. High-energy ball milling (HEBM) and mechanical alloying (MA) have been clearly established as processing techniques to prepare large quantities of nanostructured materials [5], including materials likely to address the issue of hydrogen storage [2-6]. In the present work we report the production of nanocrystalline Mg-Zn alloys by MA and their microstructural characterization. These alloys represent a first stage in our work to develop optimized Mg-base materials for hydrogen storage applications.

2. Experimental

Powder mixtures of elemental Mg and Zn powders, with nominal purity of 99.8 and 99.9%; respectively, were subjected to MA by using a high-energy ball mill (Fritsch P-6) run at 350 rpm. The particle size of the elemental powders was <500 μm and <100 μm, respectively. All milling experiments were performed in stainless steel vials of 500 ml capacity filled and closed in a glove box under Ar atmosphere.

In order to obtain nanocrystalline Mg-Zn alloyed powders, the following process parameters were varied: ball-to-powder mass ratio (b/p), milling time, number and mass of the individual balls and quantity of process control agent (PCA). The optimized milling conditions found in our experiments are indicated in Table I. Methanol (3 ml) was used as PCA during mechanical alloying. Qualitative phase characterization of the as-milled powders at various stages of MA processing was carried out by x-ray diffraction (XRD) using CoKα radiation and a graphite monochromator on the path of the diffraction beams. Powder size and morphology and average chemical composition were determined by scan-

ning electron microscopy (SEM) and energy-dispersive x-ray spectrometry (EDXS), respectively. The latter was performed on powders glued, as densely as possible, to graphite cloth. Transmission electron microscopy (TEM) was used to assess the nanocrystalline structure of the as-milled materials. Also, a Rietveld analysis of the XRD data has been performed to estimate the lattice parameters of as-milled Mg and mechanically alloyed Mg-Zn materials.

3. Results and discussion

3.1. Characterization of the as-received powders

XRD patterns from the as-received Zn and Mg powders are shown in Figures 1a and 1b, respectively. Figure 1a shows only Bragg reflections from Zn; their positions and relative intensities are in good agreement with the standard values (ICSD Collection Code 4-0831). In turn, in the XRD pattern from the Mg powders (Fig. 1b) only diffraction peaks from Mg are detected with positions and relative intensities well in agreement with the standard values (ICSD Collection Code 35-0821). It should be noticed that no diffraction peaks from the corresponding oxides are evident in the diffraction patterns in Figs. 1a and 1b.

The average chemical composition of the as-received elemental powders, as measured by EDXS in the SEM, reported

TABLE I. Optimized experimental milling conditions

Sample	Milling time, h	b/p	Nominal composition
A	30	11	Mg+5wt.% Zn
B	60	11	Mg+0wt.% Zn
C	60	11	Mg+5wt.% Zn
D	60	11	Mg+10wt.% Zn

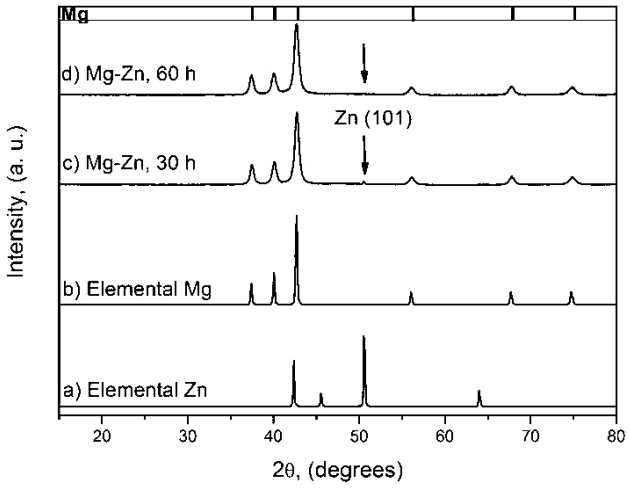

FIGURE 1. XRD patterns from (a) Zn, (b) Mg, (c) Mg + 5 wt.% Zn ball-milled for 30 h and (d) Mg + 5 wt. % Zn ball-milled for 60 h.

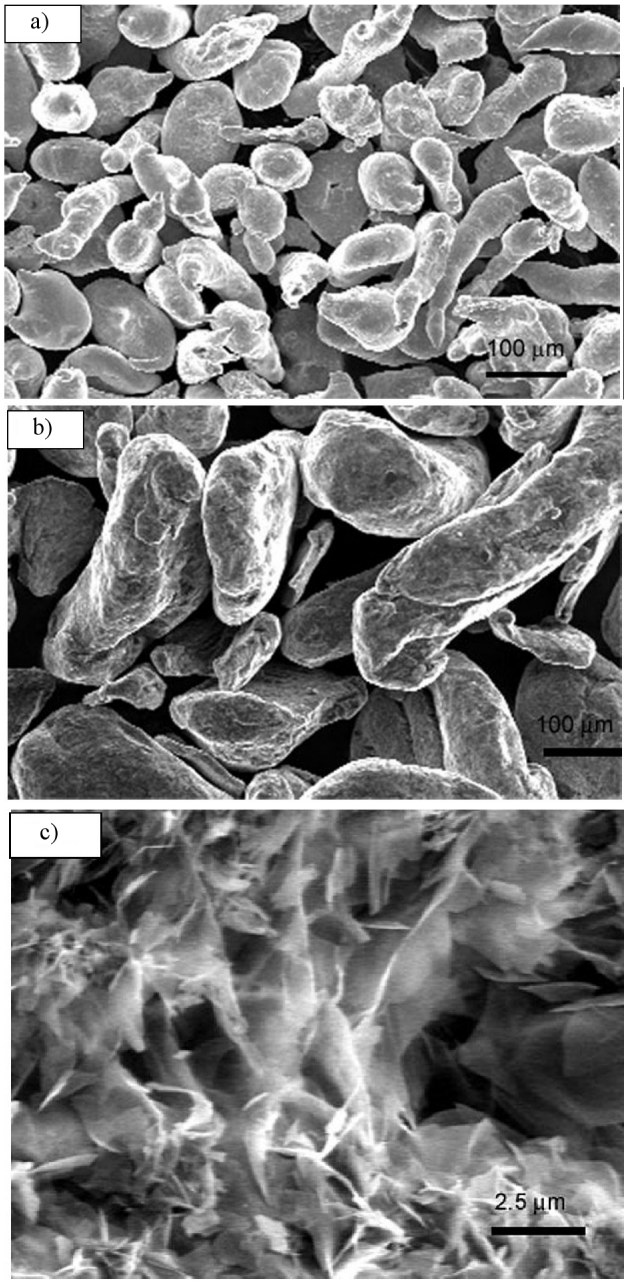

FIGURE 2. SEM micrographs of the as-received powders of: (a) Zn, (b) Mg and (c) Mg (at higher magnification).

an oxygen content of about 3 and 20 wt.% in Zn and Mg powders, respectively. Although quantitative oxygen determinations by EDXS are not particularly accurate, these values serve as a rough comparison of the conditions of the starting materials. SEM micrographs of the starting Zn and Mg powders are shown in Figures 2a to 2c. Zn powders are mostly ellipsoidal, elongated particles of sizes up to 250 μm (Fig. 2a). A more massive morphology can be observed for the Mg powders, with a particle size between 100 and 500 μm (Fig. 2b).

From SEM observations it was found that the surface of the Mg powders was covered by thin flakes of magnesium oxide or hydroxide (Fig. 2c). The reduced thickness of the oxi-

dized layer may explain the absence of diffraction peaks from the oxide phase in the corresponding XRD pattern (Fig. 1b), as x-rays would diffract rather weakly from thin oxide layers. On the other hand, characteristic oxygen x-rays from this surface oxide would be more easily detected by EDXS since they would be weakly absorbed before arriving at the x-ray detector (and the corresponding calculation of oxygen content would be overestimated).

3.2. Characterization of the mechanically alloyed powders

Mixtures of Mg containing 5 wt.% Zn were subjected to MA for different periods of time. The corresponding XRD patterns of the as-milled powders are shown in Figs. 1c and 1d. After 30 h of MA only the strongest Zn reflection (101) is still evident (Fig. 1c), along with those from Mg. This means that complete alloying between Mg and Zn has not been yet accomplished. However, considerable broadening of all diffraction peaks is evident indicating a decrease in crystallite size (probably below 100 nm) and the existence of microstrains (typically produced in highly deformed metallic powders). No reflections from any other phase are present in the XRD patterns from the as-milled powders. Figure 1d shows the XRD pattern from a sample ball-milled for 60 h. In this case only Bragg reflections from Mg are evident, indicating that alloying of the Mg and Zn powders has achieved a more advanced stage. Here again, microstrains and/or nanometric crystallite sizes can be inferred from the observed broadening of the diffraction peaks.

In passing, it should be noticed that no diffraction peaks from iron are observed in the XRD patterns from the as-milled powders. This is a first indication that contamination from the milling device did not occur to a significant level. This was further confirmed by the results of EDXS analysis, as illustrated in Fig. 3. EDXS of the as-milled powders reported Zn contents of about 4.8 and 5.2 wt.% in Mg + 5 wt.% Zn milled for 30 and 60 h, respectively, in good agreement with the nominal Zn content.

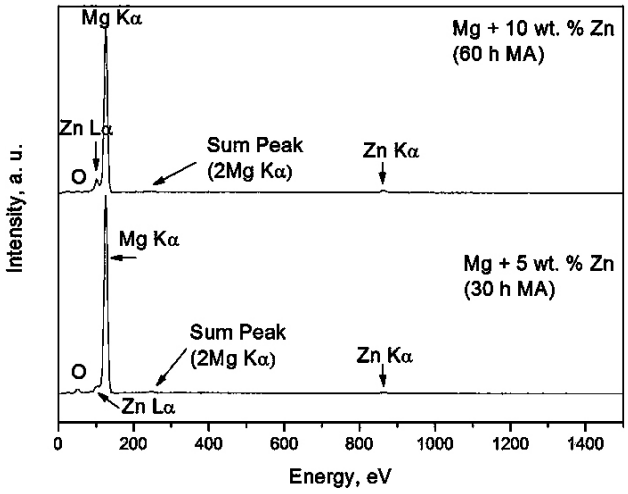

FIGURE 3. EDS spectra from Mg + 5 wt.% Zn and Mg + 10 wt.% Zn after MA.

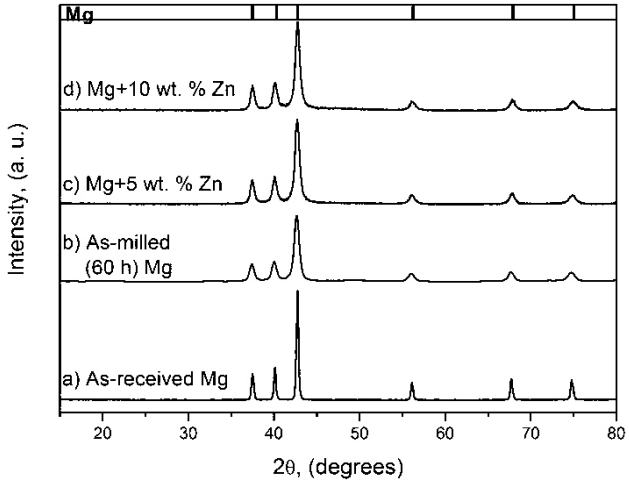

FIGURE 4. XRD patterns from: (a) as-received and (b) as-milled (60 h) Mg and as-milled (60 h) (c) Mg + 5 wt.% Zn and (d) Mg + 10 wt.% Zn.

Powder samples with 0 and 10 wt.% Zn content were also milled for 60 h (see Table 1). The XRD patterns from samples milled for 60 h are shown in Fig. 4. Comparing the XRD patterns of as-received (Fig. 4a) and as-milled (Fig. 4b) samples it becomes again evident that a significant decrease in crystallite size took place after 60 h of milling, judging by the broadening of the diffraction peaks, although a microstrain component of the broadening should also be present.

The XRD pattern corresponding to a Mg + 5 wt.% Zn sample milled for 60 h is shown in Fig. 4c. From this figure it is clear that complete alloying between the original elemental powders was achieved after 60 h of MA, judging by the absence of the strongest Zn reflection (101). In fact, this figure and the one corresponding to pure Mg milled for the same period of time (Fig. 4b) are apparently quite similar, exhibiting only the Mg phase. Figure 4c also shows a considerable broadening of the Mg diffraction peaks.

Increasing the Zn content to 10 wt.% seems to have no effect on the nature of the phases produced after MA for 60 h. This is illustrated by the XRD pattern in Fig. 4d, in which, again, only Mg reflections occur, suggesting the complete dissolution of Zn in the Mg matrix.

The Mg-Zn equilibrium phase diagram indicates a maximum solubility of Zn in Mg of about 7 wt.% [7]. The difference between the equilibrium solubility (7 wt.%) and the largest amount of Zn apparently dissolved in the samples processed by MA (10 wt.% Zn) can be explained by the well-known tendency of the mechanically alloyed materials to form metastable, extended solid solution phases [5].

Lattice parameters of the as-milled powders have been determined by Rietveld analysis of the XRD data shown in Figs. 4b-d. A difference of about 0.07-0.08% was found in the lattice parameters determined for as-milled (60 h) pure Mg with respect to the standard values (ICSD Collection Code 35-0821). Lattice parameters of Mg-Zn powder mixtures containing 0.5 and 10 wt.% Zn after 60 h of MA pro-

cessing are indicated in Table II. As expected, the lattice parameters of the Mg-Zn solid solutions decrease with increasing Zn content, since Zn atoms are smaller than Mg atoms (atomic radii: 1.38 and 1.60 Å, respectively [8]).

The relative differences between the lattice parameters values of as-milled pure Mg and as-milled Mg + 5 and 10 wt.% Zn powder mixtures are also shown in Table II. The Mg + 5 wt.% Zn sample shows a decrease of $\sim$ 0.14 - 0.15% in the lattice parameter values, while the corresponding decrease calculated from equilibrium data [9] is about 0.28% (parameter a) and 0.17 (parameter c) for 5 wt.% Zn in solid solution. Notice, however, that this Zn content in *equilibrium* solid solution is attained at a temperature of about 290 °C. Similarly, the lattice parameters of the Mg + 10 wt.% Zn sample exhibit a decrease of $\sim$ 0.23 - 0.27% after milling for 60 h; however, although no data is available for equilibrium Mg-Zn solid solutions with Zn content larger than about 7.5 wt.%, already the relative changes reported for this Zn content (at 340°C [9]) are 0.42% (parameter a) and 0.32% (parameter c), *i.e.*, larger than the changes determined in the Mg + 10 wt.% Zn sample. The main conclusion from this analysis is that some amount of Zn has indeed been dissolved in Mg by mechanical alloying and that the amount is about two times larger in the Mg + 10 wt.% Zn sample compared to the Mg + 5 wt.% Zn sample. Because of their nanocrystalline structure, it is more difficult to assess the exact amount of Zn which actually exists in solid solution in the mechanically alloyed samples. Due to the much higher density of lattice defects (including, grain boundaries, dislocations, point defects) present in nanocrystalline materials produced by MA, solubility may be enhanced with a diminished effect on the lattice volume, as the solute atoms can be more easily accommodated in a defective structure. As a consequence, one can not calculate the amount of Zn dissolved in Mg in the mechanically alloyed products by directly comparing their lattice parameter values to those of conventional (polycrystalline) Mg-Zn solid solutions (as reported in Ref. 9). In any case, considering that the maximum Zn content in Mg at room temperature is about 2 wt.% [9], it turns out that the observed changes in the mechanically alloyed samples indicate that in both powder alloys *metastable* Mg-Zn solid solutions were indeed obtained.

The morphology of the mechanically alloyed powders is shown in Figs. 5a and 5b. A SEM micrograph of a Mg + 5 wt.% Zn sample milled for 30 h is shown in Fig. 5a, in which granular particles of 1-10 μm in size stick together to form larger agglomerates. By comparing to the as-received powders (Figs. 2a and 2b), morphology changes as well as particle size reduction are evident after MA. The homogeneity of the mechanically alloyed materials is also evident, judging by the flat compositional contrast observed after 60 h of HEBM in Fig. 5b. This figure shows an SEM micrograph using compositional contrast (backscattered electron image) from the Mg + 10 wt.% Zn sample ball-milled for 60 h.

TEM observations confirm the refinement of the microstructure within the powder particles due to MA processing. A dark field TEM image of as-milled Mg powders is shown in Fig. 6a. Crystallites less than 20 nm in size are seen in this figure. A selected–area electron diffraction (SAED) pattern from the particle shown in Fig. 6a is provided in Fig. 6b. This SAED pattern exhibits continuous diffraction rings which can be indexed as belonging to elemental magnesium, magnesium hydroxide and MgO.

A TEM image from the Mg + 5 wt. % Zn sample after MA for 30 h is shown in Fig. 7a, in which nanocrystalline diffraction domains of less than 20 nm in size are again seen. The corresponding SAED pattern (Fig. 7b) indicated the presence of Zn, Mg and MgO (and perhaps $Mg_3O_2(OH)_2$). Also, the nanocrystalline structure suggested by the broadening in the corresponding x-ray diffraction patterns (Fig. 4d) of the Mg + 10 wt. % Zn sample ball-milled for 60 h is confirmed in the TEM micrograph shown in Figure 7c. The presence of Mg, MgO and probably $Mg_3O_2(OH)_2$ was also detected by SAED (Fig. 7d), but no diffraction rings could be ascribed to Zn; this observation agrees with the formation of a solid solution between the elemental Mg and Zn powders.

TABLE II. Lattice parameters of Mg and Mg-Zn solid solutions determined by Rietveld analysis and relative changes with respect to Mg.

Parameters	Mg+ 0Zn	Mg+ 5Zn	% Diff.	Mg+ 10Zn	% Diff.
a=b, nm	0.32116	0.32067	0.15	0.32043	0.23
c,nm	0.52146	0.52071	0.14	0.52007	0.27

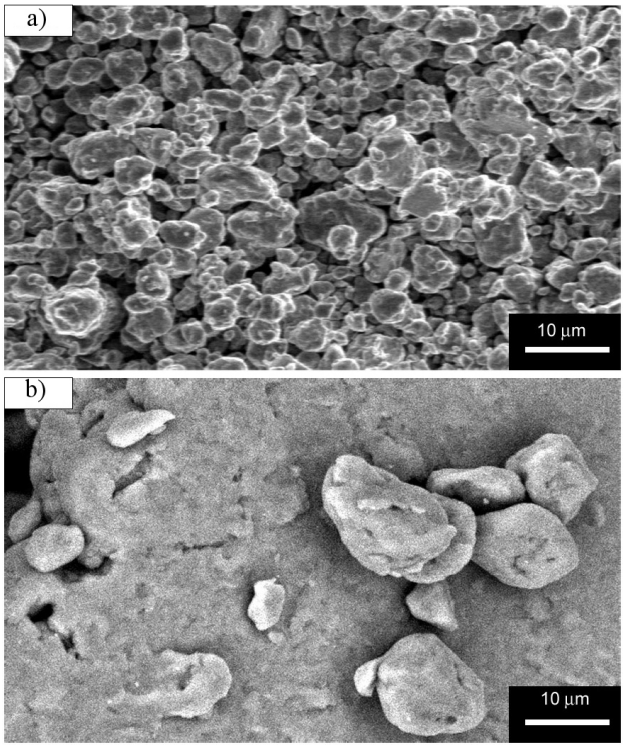

FIGURE 5. SEM micrographs of as-milled powder samples. (a) Mg + 5 wt.% Zn (30 h) and (b) Mg + 10 wt.% Zn (60 h).

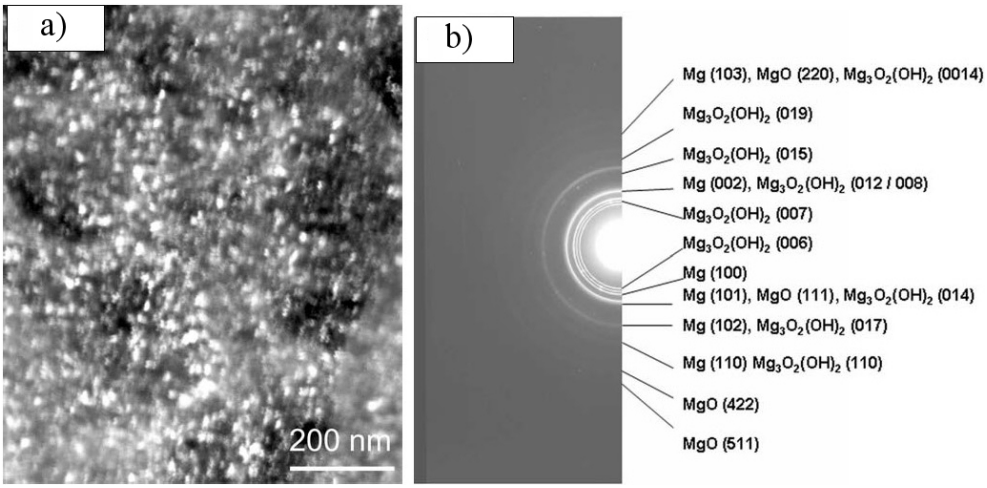

FIGURE 6. (a) Dark field TEM image of Mg powders milled for 60 h. (b) Corresponding SAED pattern.

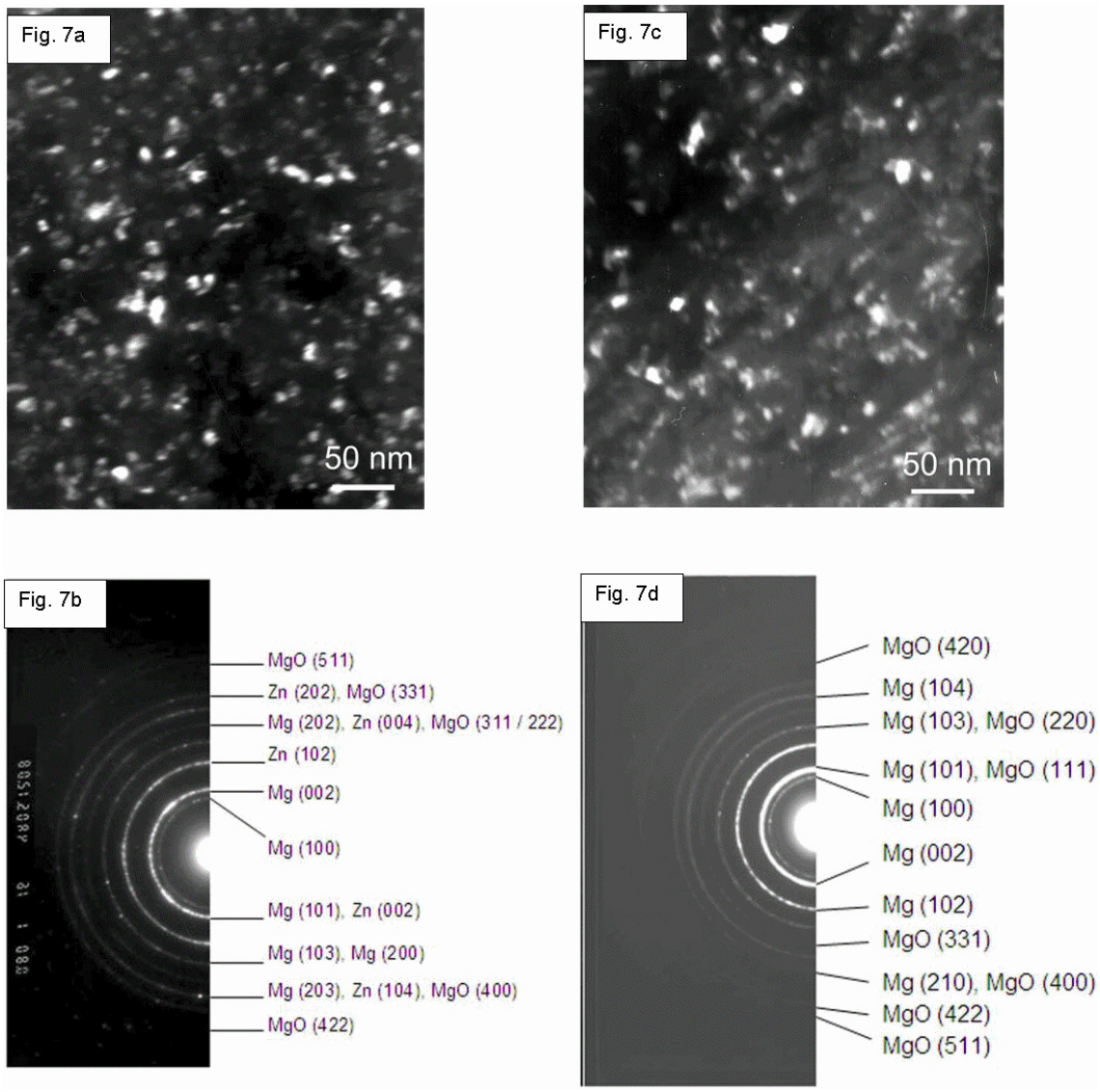

FIGURE 7. Dark field TEM images of (a) Mg + 5 wt.% Zn milled for 30 h and (c) Mg + 10 wt.% Zn milled for 60 h. Corresponding SAED patterns (b) and (d).

4. Conclusions

Elemental Mg and Zn powder samples with different Zn content were subjected to MA. After 30 h of ball-milling, traces of elemental Zn were still present, whereas "complete" alloying was evident after 60 h of MA. A rather homogeneous structure consisting of nanocrystalline domains of less than 20 nm in size was found in all the mechanically alloyed powders. The amount of Zn in the mechanically alloyed powders had the effect of decreasing the values of the lattice parameters of the hexagonal unit cell of Mg, in agreement with the literature regarding conventional, polycrystalline Mg-Zn alloys. The measured changes in lattice parameters indicate that the materials produced were metastable Mg-Zn solid solutions. The mechanically alloyed materials which have been produced are to be tested as candidate hydrogen storage alloys.

Acknowledgements

The authors wish to express their gratitude to Dr. A. Sandu of Toyohashi University of Technology, Japan, for his help with the TEM measurements. Work partially supported by IPN (project 20060809) and CONACYT (project SEP-2004-C01-48045/A-1) in Mexico and the AIEJ program in Japan. AFPL and JLLS gratefully acknowledge PIFI-IPN scholarships. AFPL gratefully acknowledges a JASSO scholarship as well. FCG and JGCM are recipients of COFAA-IPN fellowships.

∗ Corresponding author.

1. S. Dunn, *Int. J. Hydrogen Energy* **27** (2002) 235.
2. G. Liang, *J. Alloys Compd.* **370** (2004) 123.
3. O. Gutfleisch *et al.*, *J. Alloys Compd.* **356-357** (2003) 598.
4. A. Zaluska, L. Zaluski, and J.O. Ström-Olsen, *J. Alloys Compd.* **288** (1999) 217.
5. C. Suryanarayana, *Prog. Mater Sci.* **46** (2001) 6.
6. A. Palacios-Lazcano, J.G. Cabañas-Moreno, and F. Cruz-Gandarilla, *Scripta Mater.* **52** (2005) 571.
7. "Binary Alloy Phase Diagrams", 2^{nd} Edition, eds. T. Massalski, H. Okamoto, P.R. Subramanian, L. Kacprzak, *ASM International* (New York, 1992) Vol. 3, p. 2572.
8. M. Winter, *The University of Sheffield* http://www.webelements.com/webelements/index.html
9. W.B. Pearson, *A Handbook of Latice Spacings and Structures of Metals And Alloys* (International Series of Monographs on Metal Physics and Physical Metallurgy / vol 4, G.V. Raynor, Editor, Pergamon Press, North Ireland, 1958), p. 728.